Japanese Journal of Radiology (2019) 37:315–320
https://doi.org/10.1007/s11604-019-00810-w

ORIGINAL ARTICLE

Liver fibrosis assessment using 99mTc-GSA SPECT/CT fusion imaging

Ryotaro Tokorodani[1,6] · Tatsuaki Sumiyoshi[2] · Takehiro Okabayashi[2] · Yasuhiro Hata[3] · Yoshihiro Noda[3] · Sojiro Morita[3] · Hiromitsu Daisaki[4] · Yukinori Okada[5] · Eisuke Yasuda[6]

Received: 4 December 2018 / Accepted: 9 January 2019 / Published online: 17 January 2019
© Japan Radiological Society 2019

Abstract

Purpose To determine the utility of mean standardized uptake value (SUV_{mean}) of whole liver measured by ^{99m}Tc-GSA SPECT/CT fusion imaging, for evaluation of liver fibrosis.

Materials and methods Eighty-six patients who underwent hepatectomy were enrolled, and were classified into the non-fibrosis or fibrosis group based on the pathological findings in the resected liver specimen. Univariate and multivariate analyses were performed between the two groups on four blood biochemical indices (albumin, total bilirubin, platelet count, and prothrombin time activity) and two ^{99m}Tc-GSA scintigraphy-derived liver function indices (LHL_{15} and SUV_{mean}) to evaluate the independent predictive value for severe fibrosis. The diagnostic value of the index for severe fibrosis was assessed by calculating the area under the receiver operating characteristic curve.

Results Multivariate analysis showed that prothrombin time activity [odds ratio (OR) 0.519], LHL_{15} (OR 0.513), and SUV_{mean} (OR 0.168) significantly correlated with liver fibrosis. SUV_{mean} showed the largest area under the curve, with value of 0.804, 0.730 for platelet count, 0.717 for LHL_{15}, and 0.668 for prothrombin time activity. The optimal cut-off value for SUV_{mean} was 6.7, which yielded 62.9% sensitivity and 96.9% specificity.

Conclusions SUV_{mean} measured by ^{99m}Tc-GSA SPECT/CT fusion imaging enables highly accurate prediction of severe liver fibrosis.

Keywords Liver fibrosis · Tc-99m-diethylenetriamine-penta-acetic acid-galactosyl human serum albumin single-photon-emission computed tomography · Standardized uptake value

Introduction

Degree of fibrosis is an important indicator of liver function, as damage to the organ leads to fibrotic change in the liver parenchyma. Cirrhosis represents the most advanced stage of liver fibrosis, which is associated with a potential risk of malnutrition, coagulopathy, and fatal liver failure, thereby posing restrictions in performing invasive therapeutic procedures [1–4]. Therefore, assessment of the degree of fibrosis is important to decide the treatment strategy for patients with liver diseases. The gold standard of assessment of liver fibrosis is biopsy; however, a non-invasive substitute diagnostic modality has not been established.

Tc-99m-diethylenetriamine-penta-acetic acid-galactosyl human serum albumin (99mTc-GSA) single-photon emission computed tomography (SPECT)/CT fusion imaging has been routinely used in the evaluation of whole and regional liver functions prior to hepatectomy at this institution [5]. The present study investigated the potential utility of the

✉ Tatsuaki Sumiyoshi
tasu050520@yahoo.co.jp

1 Department of Radiological Technology, Kochi Health Sciences Center, Kochi, Japan

2 Department of Gastroenterological Surgery, Kochi Health Sciences Center, 2125 Ike, Kochi, Japan

3 Department of Radiology, Kochi Health Sciences Center, Kochi, Japan

4 Department of Gunma Prefectural College of Health Sciences, Maebashi, Japan

5 Department of Radiology, St. Marianna University School of Medicine, Kawasaki, Japan

6 Department of Radiological Technology, Graduate School of Health Science, Suzuka University of Medical Science, Suzuka, Japan

technique in the evaluation of liver fibrosis. 99mTc-GSA is exclusively taken up by the liver and specifically binds to asialoglycoprotein receptor on hepatocytes, and a decreased number of receptors are observed in patients with liver damage [6, 7]. Therefore, ^{99m}Tc-GSA scintigraphy enables the direct estimation of functioning hepatocytes and is an excellent method for the evaluation of regional and whole liver function [8].

These previous reports used the ratio of liver to heart-plus-liver radioactivity for 15 min (LHL_{15}) value, which is representative for whole liver function index of 99mTc-GSA scintigraphy; one previous report described that LHL_{15} value showed a significant correlation with the degree of liver fibrosis [9]. However, LHL_{15} is detected by planar image of ^{99m}Tc-GSA scintigraphy; therefore, is deficient in the three-dimensional depth direction information (Fig. 1a) [10].

A recent study reported highly accurate attenuation correction, scatter correction, and resolution correction to enable the quantification using standardized uptake value (SUV) [11]. SUV depicts the degree of accumulation of radiopharmaceutical substances in the target organ, and enables obtaining three-dimensional depth direction information [12]. Therefore, it was assumed that SUV might demonstrate better correlation with liver fibrosis than LHL_{15}. The concept of SUV was applied to 99mTc-GSA scintigraphy for the first time in this study, and the value of this indicator was investigated in the evaluation of liver fibrosis.

Methods

Patients

Eighty-six patients who underwent hepatectomy between September 2014 and September 2017 were enrolled in the retrospective study. All patients underwent ^{99m}Tc-GSA SPECT/CT fusion imaging prior to the hepatectomy to evaluate whole and regional liver functions. The study was approved by the institutional review board, with waiver of informed consent.

Blood biochemistry (liver function tests)

The values of four blood biochemical indices (albumin, total bilirubin, platelet count, and prothrombin time activity) prior to the hepatectomy were investigated.

^{99m}Tc-GSA SPECT/CT fusion imaging

^{99m}Tc-GSA SPECT/CT fusion imaging has been routinely applied at our institution, in hepatectomy candidates to evaluate liver function. All patients underwent the examination with a Symbia T6 scanner (Siemens, Munich, Germany). This instrument combines variable angle dual detector SPECT with 6-slice CT for rapid, accurate attenuation correction and precise localization. The instrument also enables the seamless transition from a SPECT examination to a CT examination, and both SPECT and CT images could be obtained in a single examination without the need for change in position. The procedure of the investigation was as follows. After overnight fasting, the patient was placed in a supine position. Cardiac and respiratory synchronization were not used in this modality. Instead, to minimize the possibility of occurrence of artifacts due to cardiac pulsation and respiratory motion, the patients were encouraged to rest and take a small, slow breath before image acquisition. 99mTc-diethylenetriamine-penta-acetic acid-GSA (Nihon Medi-Physics, Tokyo, Japan) (185 MBq/3 mg) was injected into an antecubital vein. SPECT data acquisition (60 steps of 20 s/step, 360°, 128 × 128 matrix) was started 20 min after the injection with a low-energy, high-resolution collimator; the entire study duration was approximately 30 min. The reconstruction algorithm for SPECT was three-dimensional ordered subset expectation maximization (iteration,

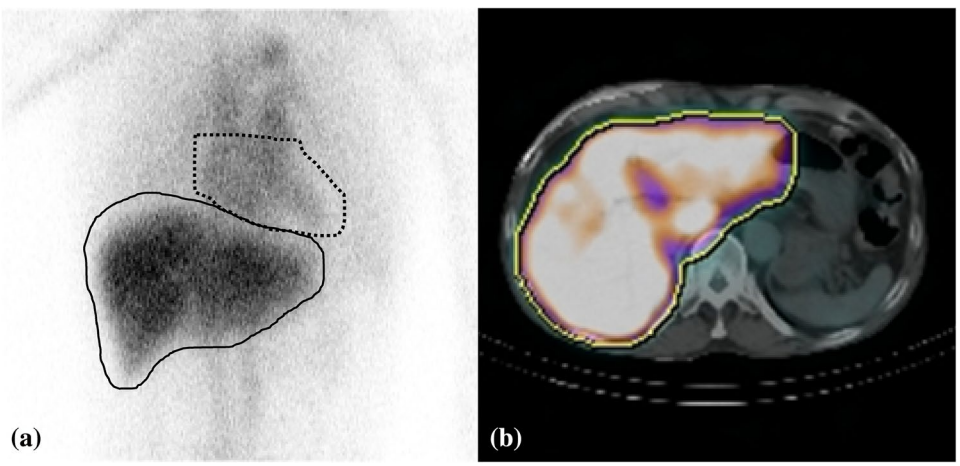

Fig. 1 Calculation of 99mTc-GSA scintigraphy-derived indices. **a** The LHL_{15} value was calculated by dividing the radioactivity of the liver ROI (solid line) by the sum of the radioactivity of the liver and heart ROIs (solid line and dot line) at 15 min post-injection. The LHL_{15} value lacks the three-dimensional depth direction information. **b** SUV_{mean} was measured by setting the volume of interest at the site of 99mTc-GSA accumulation

10; subsets, 6), with attenuation and scatter corrections. 3D Gaussian filter was used as a post-processing filter (9.6 mm full-width at half-maximum). Following SPECT examination, non-enhanced CT images were obtained under standard conditions of 130 kV, 345 mA, 12-mm table feed per rotation, 0.6-s gantry rotation time, 0.6-mm collimation, and 1-mm reconstruction. CT images were reconstructed using a standard algorithm with a 166-cm field-of-view of the target sites. The SPECT and CT images were fused automatically using the embedded Siemens common platform software Syngo MI workplace. SPECT slice data were retrieved through Digital Imaging and Communications in Medicine (DICOM), and SPECT slices were converted to a CT-like data volume for the fusion of the SPECT and CT images.

Calculation of LHL_{15}

The ROI was set by one radiological technologist and one radiologist specializing in nuclear medicine at this information on mutual consent. The LHL_{15} value was calculated by dividing the radioactivity of the liver ROI (L_{15}) by the sum of the radioactivity of the liver and heart ROIs ($L_{15} + H_{15}$) at 15 min post-injection (Fig. 1a) [13, 14]:

$$LHL_{15} = \frac{L15}{L15 + H15}.$$

Calculation of SUV_{mean}

The accumulation of 99mTc-GSA in the liver was evaluated using SUV [11]. Decay correction was applied in all patients to control the fluctuation at the start time of the acquisition. SUV value was normalized by the liver volume, which was calculated automatically using workstation VINCENT (FUJIFILM, Tokyo, Japan) [15].

SUV was calculated using the following formula:

$$SUV_{mean} = \frac{\text{Radioactivity of liver VOI (Bq/ml)}}{\text{Dose at the start of scan(Bq)/Livervolume (ml)} \times 10}.$$

Setting the volume of interest (VOI) at the site of 99mTc-GSA accumulation in the liver is necessary to calculate SUV; therefore, we applied a commercially available GI-BONE (AZE Co., Ltd., Tokyo, Japan), which is known to set VOI automatically (Fig. 1b). The VOI was placed to contain the whole liver. Then, the software automatically detected the region of voxel with SUV > 3, and the mean value of SUV in the designated region was calculated. Further, 99mTc-GSA is taken up only in the liver, not in whole body, and therefore, liver volume was utilized to normalize the radioactivity in this study.

Degree of fibrosis

Degree of fibrosis was pathologically diagnosed in the liver parenchyma apart from the liver tumor in each resected specimen. The Ludwig scale was utilized to stratify the grade of fibrosis; F1 (no fibrosis or fibrosis confined to enlarged portal tracts), F2 (periportal fibrosis or portal-to-portal septa but intact architecture), F3 (septal fibrosis with architecture distortion), and F4 (probable or definite cirrhosis). The degree of fibrosis was assessed by two pathologists who were blinded the patient characteristics. Grades F1 and F2 were classified in the non-fibrosis group, and grades F3 and F4 were classified in the fibrosis group [16]. Univariate and multivariate analysis were performed between the two groups on four blood biochemical indices and two ^{99m}Tc-GSA scintigraphy-derived liver function indices to evaluate the independent predictive value for severe fibrosis. The diagnostic value of the index for severe fibrosis was assessed by calculating the area under the receiver operating characteristic (ROC) curve.

Statistical analysis

The data were not distributed normally. Therefore, median values and non-parametric statistical testing procedures were utilized. The Mann–Whitney *U* test was used for continuous variables, and the chi-square test was used for categorical variables. Differences between medians were considered statistically significant at p value of < 0.05. Significant variables obtained by univariate analysis were entered simultaneously (forced entry method) into multivariate logistic regression analysis to evaluate their independent predictive value for severe fibrosis. The diagnostic value of the index was assessed by calculating the area under the ROC curve. These statistical analyzes were performed using SPSS 24 for Windows (SPSS, Chicago, IL, United States).

Results

Clinical characteristics

The clinical characteristics of the patients included in this study ($n = 86$) are described in Table 1. The patient population comprised of 36 males and 15 females with a median age of 72 years (range 42–86 years) in the non-fibrosis group. The fibrosis group comprised 25 males and 10 females with a median age of 74 years (range 39–86 years), and no significant differences were observed between the two groups (Table 1). The body weights in both groups were also equivalent. The positive rates of hepatitis B, hepatitis C, alcohol abuse, and non-alcoholic steatohepatitis showed no significant differences between the two groups (Table 1).

Table 1 Clinical characteristics of the non-fibrosis and fibrosis groups

	Non-fibrosis ($n=51$)	Fibrosis ($n=35$)	p value
Gender (male/female)	36/15	25/10	0.868
Age range (median)	42–86 (72)	39–86 (74)	0.786
Body weight (kg)	56.15	58.5	0.876
Hepatitis B (±)	8/43	4/31	0.542
Hepatitis C (±)	11/40	12/23	0.135
Alcohol abuse (±)	8/43	6/29	0.831
NASH (±)	1/50	3/32	0.162

NASH non-alcoholic steatohepatitis

Comparison of liver function index between non-fibrosis and fibrosis groups

Results of univariate and multivariate analyses are summarized in Table 2. In univariate analysis, the median value of serum albumin (g/dL), total bilirubin (g/dL), platelet count ($\times 10^4/mm^3$), and prothrombin time activity (PT%) were 4.2 vs. 3.9 ($p=0.272$), 0.6 vs. 0.7 ($p=0.057$), 17.6 vs. 12.9 ($p<0.001$), and 96.5 vs. 86.7 ($p=0.009$), respectively, between the non-fibrosis and fibrosis groups. The platelet count and PT% showed significant differences between the two groups. The median value of LHL_{15} and SUV_{mean} were 0.917 vs. 0.874 ($p<0.001$) and 6.8 vs. 6.0 ($p<0.001$), respectively, and both the 99mTc-GSA scintigraphy-derived indices showed significant differences between the two groups. In these indices, multivariate analysis showed that PT% (OR 0.519), LHL_{15} (OR 0.513) and SUV mean (OR 0.168) significantly correlated with liver fibrosis.

Diagnostic value of indices for liver fibrosis

ROC curves were constructed and AUCs were compared on four variables: platelet count, PT%, LHL15, and SUV_{mean} (Fig. 2). The AUCs were 0.804 for SUV_{mean}, 0.730 for platelet count (vs. SUV_{mean}, $p=0.249$), 0.717 for LHL15 (vs. SUV_{mean}, $p=0.084$), and 0.668 for PT% (vs. SUV_{mean}, $p=0.075$). Although statistical significances of AUCs were not observed between SUV_{mean} and other three variables, SUV_{mean} showed the largest AUC. The optimal cut-off value for SUV_{mean} was 6.7, which yielded 62.9% sensitivity, 96.9% specificity, 97.1% positive predictive value, and 60.8% negative predictive value.

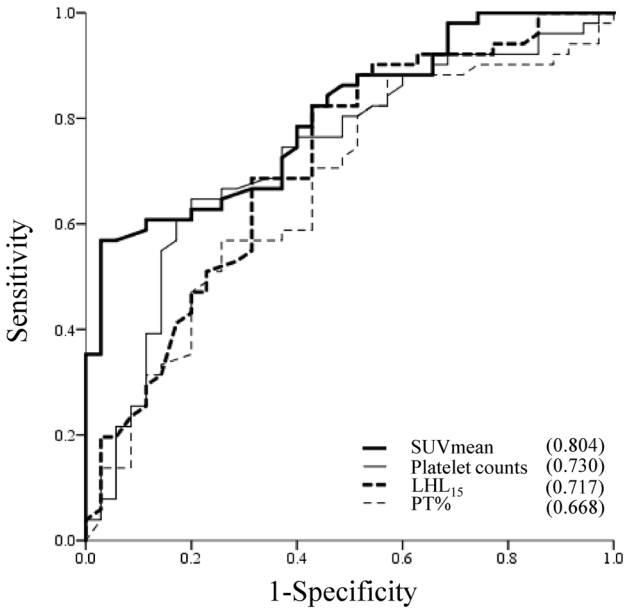

Fig. 2 The diagnostic value for severe fibrosis. AUCs were compared in four variables: platelet count, prothrombin time activity, LHL_{15}, and SUV_{mean}. SUV_{mean} showed the largest AUC

Discussion

Continuous damage to the liver leads to progression of fibrosis and eventually cirrhosis, regardless of the cause of liver damage such as hepatitis virus, alcohol, and fatty

Table 2 Comparison of liver function index between the non-fibrosis and fibrosis groups

	Univariate			Multivariate	
	Non-fibrosis	Fibrosis	p value	Odds ratio	p value
Albumin (g/dL)	4.2 (3.0–5.0)	3.9 (2.3–4.9)	0.272		
Total bilirubin (mg/dL)	0.6 (0.2–1.2)	0.7 (0.3–1.7)	0.057		
Platelet count ($\times 10^4/mm^3$)	17.6 (6.9–49.6)	12.9 (6.5–42.9)	< 0.001	0.625 (0.313–1.222)	0.166
Prothrombin time (%)	96.5 (33.6–117.7)	86.7 (51.5–117.7)	0.009	0.519 (0.258–0.824)	0.020
LHL_{15}	0.917 (0.786–0.960)	0.874 (0.687–0.950)	< 0.001	0.513 (0.278–0.947)	0.038
SUV_{mean}	6.8 (5.1–8.1)	6.0 (3.2–7.1)	< 0.001	0.168 (0.048–0.435)	< 0.001

Number in non-fibrosis and fibrosis groups shows the median value. Number in the parentheses shows range of the value

liver [3]. Patients with cirrhosis have a potential risk of fatal liver failure; therefore, assessment of fibrosis is crucial to decide the treatment strategy for patients with liver diseases. Liver biopsy, which is the gold standard for assessing fibrosis, is an invasive technique and is associated with limitations such as bleeding and/or sampling error [17]. Non-invasive indicators, such as hyaluronic acid, procollagen III peptide, and type IV collagen [18–22], are effective markers of fibrosis; however, these markers are not specific to the liver.

Therefore, the present study investigated the utility of 99mTc-GSA scintigraphy in the evaluation of liver fibrosis. A previous study reported that LHL_{15} value of 99mTc-GSA scintigraphy showed a significant correlation with the degree of liver fibrosis [9]. However, LHL_{15} lacks the three-dimensional depth direction information, as the index is calculated from planar scintigraphic images, which do not accurately reflect hepatocyte volume. To overcome this problem, SUV was applied in 99mTc-GSA scintigraphy for the first time in this study. The concept of SUV is widely applied and commonly used in the field of positron-emission tomography scan, and the quantified value facilitates evaluation of the target organ. SUV could be accurately and automatically measured from 99mTc-GSA SPECT/CT fusion imaging using GI-BONE.

Several liver function indices were compared between the fibrosis and non-fibrosis groups in this study. Multivariate analysis revealed that PT%, LHL_{15}, and SUV_{mean} showed significant discrepancies between the two groups, and the OR was smallest in SUV_{mean}. Further, ROC curve revealed that SUV_{mean} was the most accurate index for diagnosing severe fibrosis. This significant correlation between SUV_{mean} and liver fibrosis was estimated to be attributed to the following reasons: 1. 99mTc-GSA has the specific nature of being taken up exclusively by the liver, and the decrease in number of functioning hepatocytes due to severe fibrosis was reflected as decreased accumulation of 99mTc-GSA in the liver, and 2. accurate assessment of 99mTc-GSA accumulation in the liver was obtained by applying SUV.

Despite the apparent utility of SUV in assessing liver fibrosis, this study has a number of limitations. The major drawback of ^{99m}Tc-GSA scintigraphy is that this modality evaluates the functioning hepatocytes, and is not a direct technique to evaluate liver fibrosis. Therefore, further investigations are necessary to elucidate the mechanism of the strong correlation of liver fibrosis and SUV_{mean} of ^{99m}Tc-GSA scintigraphy. Second, there is no clinical availability of ^{99m}Tc-GSA in western countries, although many studies have been published using this radiopharmaceutical agent in Japan and some countries. Third, the correlation between SUV_{mean} and long-term prognosis was estimated to enhance the clinical utility of this study. However, we could not investigate the correlation, because 86 patients in this study were candidates for hepatectomy, and the prognoses were strongly influenced by each hepatic tumor.

In conclusion, SUV_{mean} of ^{99m}Tc-GSA scintigraphy enables highly accurate prediction of severe liver fibrosis.

Funding We received no financial support.

Compliance with ethical standards

Conflict of interest We have no conflict of interest to declare.

Ethical approval All procedures performed in studies involving human participants were in accordance with the ethics committee of the Kochi Health Sciences Center and with the 1964 Helsinki declaration. The study was approved by the institutional review board of Kochi Health Sciences Center, with a waiver of informed consent.

References

1. Farges O, Malassagne B, Flejou JF, Balzan S, Sauvanet A, Belghiti J. Risk of major liver resection in patients with underlying chronic liver disease: a reappraisal. Ann Surg. 1999;229:210–5.
2. Nagino M, Kamiya J, Nishio H, Ebata T, Arai T, Nimura Y. Two hundred forty consecutive portal vein embolizations before extended hepatectomy for biliary cancer: surgical outcome and long-term follow-up. Ann Surg. 2006;243:364–72.
3. Zarzavadjian A, Bian L, Costi R, Sbai-Idrissi MS, Smadja C. Liver resection and metabolic disorders: an undescribed mechanism leading to postoperative mortality. World J Gastroenterol. 2014;20:55–62.
4. Wang Q, Fiel M, Blank S, Luan W, Kadri H, Kim KW, et al. Impact of liver fibrosis on prognosis following liver resection for hepatitis B-associated hepatocellular carcinoma. Br J Cancer. 2013;109:573–81.
5. Sumiyoshi T, Shima Y, Okabayashi T, Noda Y, Hata Y, Murata Y, et al. Functional discrepancy between two liver lobes after hemilobe biliary drainage in patients with jaundice and bile duct cancer: an appraisal using 99mTc-GSA SPECT/CT fusion. Radiology. 2014;273:444–51.
6. Sobue G, Kosaka A. Asialoglycoproteinemia in a case of primary hepatic cancer. Hepatogastroenterology. 1980;27:200–3.
7. Marshall JS, Green AM, Pensky J, Williams S, Zinn A, Carlson DM. Measurement of circulating desialylated glycoproteins and correlation with hepatocellular damage. J Clin Investig. 1974;54:555–62.
8. Okabayashi T, Shima Y, Morita S, Shimada Y, Sumiyoshi T, Sui K, et al. Liver function assessment using technetium 99m-Galactosyl single-photon emission computed tomography/CT fusion imaging: a prospective trial. J Am Coll Surg. 2017;225:789–97.
9. Okabe H, Beppu T, Hayashi H, Mima K, Nakagawa S, Kuroki H, et al. Rank classification based on the combination of indocyanine green retention rate at 15 min and (99m) Tc-DTPA-galactosyl human serum albumin scintigraphy predicts the safety of hepatic resection. Nucl Med Commun. 2014;35:478–83.
10. Hasegawa D, Onishi H. Evaluation of accuracy for quantitative predictor of hepatic functional reserve using planar and SPECT images in the 99mTc-GSA scintigraphy. Nihon Hoshasen Gijutsu Gakkai Zasshi. 2017;73:1055–60.
11. Suh MS, Lee WW, Kim YK, Yun PY, Kim SE. Maximum standardized uptake value of 99mTc hydroxymethylene diphosphonate

SPECT/CT for the evaluation of temporomandibular joint disorder. Radiology. 2016;280:890–6.
12. Kinahan PE, Fletcher JW. Positron emission tomography-computed tomography standardized uptake values in clinical practice and assessing response to therapy. Semin Ultrasound CT MR. 2010;31:496–505.
13. Kokudo N, Vera DR, Makuuchi M. Clinical application of TcGSA. Nucl Med Biol. 2003;30:845–9.
14. Kwon AH, Ha-Kawa SK, Uetsuji S, Kamiyama Y, Tanaka Y. Preoperative regional maximal removal rate of technetium-99m-galactosyl human serum albumin (GSA-Rmax) is useful for judging the safety of hepatic resection. Surgery. 1995;117:429–34.
15. Oshiro Y, Ohkohchi N. Three-dimensional liver surgery simulation: computer-assisted surgical planning with three-dimensional simulation software and three-dimensional printing. Tissue Eng Part A. 2017;23:474–80.
16. Ludwig J (1993) The nomenclature of chronic active hepatitis: an obituary. Gastroenterology 105:274–278
17. Vallet-Pichard A, Mallet V, Nalpas B, Verkarre V, Nalpas A, Dhalluin-Venier V et al (2007) FIB-4: an inexpensive and accurate marker of fibrosis in HCV infection. Comparison with liver biopsy and fibrotest. Hepatology 46:32–36
18. Jabor A, Kubíček Z, Fraňková S, Šenkeříková R, Franeková J. Enhanced liver fibrosis (ELF) score: Reference ranges, biological variation in healthy subjects, and analytical considerations. Clin Chim Acta. 2018;483:291–5.
19. Gudowska M, Cylwik B, Chrostek L. The role of serum hyaluronic acid determination in the diagnosis of liver fibrosis. Acta Biochim Pol. 2017;64:451–7.
20. Khan S, Subedi D, Chowdhury UMM (2006) Use of amino terminal type III procollagen peptide (P3NP) assay in methotrexate therapy for psoriasis. Postgrad Med J 82:353–354
21. Murawaki Y, Ikuta Y, Nishimura Y, Koda M, Kawasaki H. Serum markers for connective tissue turnover in patients with chronic hepatitis B and chronic hepatitis C: a comparative analysis. J Hepatol. 1995;23:145–52.
22. Bulatova IA, Schekotova AP, KrivtsovAV, Schekotov VV, Pavlov AI (2015) The noninvasive evaluation of degree of expression of fibrosis of liver and significance of polymorphism of gene of hyaluronic acid under chronic hepatitis C. Klin Lab Diagn 60:18–21

Publisher's Note Springer Nature remains neutral with regard to jurisdictional claims in published maps and institutional affiliations.